NASA TECHNICAL NOTE

NASA TN D-4023

PHOTOGRAPHIC STUDY OF CONDENSING MERCURY FLOW IN 0- AND 1-G ENVIRONMENTS

by David Namkoong, Henry B. Block, Robert P. Macosko, and Clifford C. Crabs

Lewis Research Center
Cleveland, Ohio

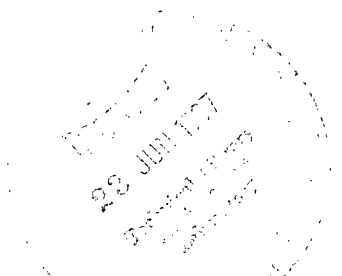

NATIONAL AERONAUTICS AND SPACE ADMINISTRATION • WASHINGTON, D. C. • JUNE 1967

NASA TN D-4023

PHOTOGRAPHIC STUDY OF CONDENSING MERCURY FLOW IN 0- AND 1-G ENVIRONMENTS

By David Namkoong, Henry B. Block, Robert P. Macosko, and Clifford C. Crabs

Lewis Research Center
Cleveland, Ohio

(Film supplement C-251 available on request)

NATIONAL AERONAUTICS AND SPACE ADMINISTRATION

For sale by the Clearinghouse for Federal Scientific and Technical Information
Springfield, Virginia 22151 – CFSTI price $3.00

PHOTOGRAPHIC STUDY OF CONDENSING MERCURY FLOW IN 0- AND 1-G ENVIRONMENTS

by David Namkoong, Henry B. Block, Robert P. Macosko, and Clifford C. Crabs

Lewis Research Center

SUMMARY

High-speed motion pictures were taken of mercury vapor condensing in glass tubes in a ground facility and in a zero-gravity facility. A range of mercury flow rates from 0.03 to 0.05 pound per second was investigated in constant-diameter tubes ranging from 0.27 to 0.49 inch. The condensing lengths were fixed at 60 and 68 inches.

Moving drops on the wall accounted for one-half or more of the liquid flow rate at any one station investigated along the condenser. The ratio of the observed average velocity of the drops in the vapor stream to the local vapor velocity varied from 0.3 at the inlet to 1.0 at approximately three-fourths of the condensing length from the inlet.

In the aircraft zero-gravity facility, the 1- and 0-g conditions had little effect on the liquid flow distribution in the 0.27-inch-diameter tube. In the 0.40- and 0.49-inch-diameter tubes, however, gravity made a substantial difference. In a 1-g environment, there was a concentration of drops on the tube bottom and a shallow sloping interface; in a 0-g environment there was a uniform distribution of drops and a vertically standing interface. Vapor pockets within the liquid leg formed and collapsed within a time interval of approximately 0.04 second.

INTRODUCTION

Many unique problems are encountered in the design of power conversion system components for space-flight applications. Among these are the behavior and associated thermodynamic and fluid dynamic characteristics of flow under weightless conditions. Knowledge of 0-g flow phenomena is of particular importance where the working fluid experiences a phase change, and the vapor and liquid flow concurrently as in the boiler and condenser components of Rankine cycle systems (e.g., SNAP-2, SNAP-8, and SNAP-50 systems).

The two-phase flow in the condenser is of particular interest because of the narrow limits imposed by adjacent turbine and circulating pump components on pressure level and pressure drop. In coasting space-flight applications where there are no gravitational forces to separate the phases, condensation is usually accomplished under forced-flow conditions. Several methods based on one of two correlations have been used for predicting pressure drop for condensing vapor flow. One method is empirical, using data based upon adiabatic, two-component flow (ref. 1). An improvement of this pressure drop correlation is given in reference 2. The other correlation is based on a flow model which assumes that all drops condensed on the tube wall become entrained in the vapor stream (ref. 3). In the flow model, it is assumed that the drops are dispersed throughout the vapor and that these drops rapidly attain the velocity of the vapor. The pressure drop correlation based on this flow model has been termed the fog-flow correlation.

Comparisons of both correlations with data are published in references 4 and 5. The data-based points, which included 0- as well as 1-g points, either diverged from the predicted curve, in one case, or scattered widely about the predicted curve in the other correlation. It is evident that observation of the flow of continuously condensing vapor is needed to confirm or modify the proposed flow models, or to establish a new model.

As part of the overall investigation of mercury condensing characteristics conducted at the NASA Lewis Research Center, high-speed motion pictures were taken of mercury condensing in glass tubes in 1- and 0-g environments. Initially, the motion pictures were taken in the ground facility to obtain visual evidence of inlet quality. This technique of observation was extended to different stations to observe condensation phenomena along the condensing length at both 1 and 0 g. In this study, not only qualitative but also quantitative information was obtained such as drop velocities and sizes. The ranges of values of mercury flow rate and tube diameter were based on the initial SNAP-8 condenser requirements. The test apparatus, with the condensing tube oriented horizontally for all tests, was operated both in the ground facility and in the AJ-2 aircraft zero-gravity flight facility (described in the appendix). Motion picture supplement C-251, which presents a detailed study of the condensing flow by extensive use of high-speed motion-picture sequences and includes results obtained in the ground facility and in the aircraft, has been prepared and is available on loan. Lewis motion picture C-221, also available on loan, describes the testing and hardware used in the AJ-2 aircraft zero-gravity flight facility and presents a few film sequences of mercury condensing in constant diameter glass tubes. A request card and a description of these films are included at the back of this report.

DESCRIPTION OF APPARATUS

The experimental system and components, instrumentation, and procedure were basically the same for tests in the ground facility and in the zero-gravity facility.

Experimental System and Components

An isometric drawing of the experimental system is presented in figure 1(a). A photograph of the basic system in an aluminum enclosure that was inserted into the aircraft is shown in figure 1(b). The experimental system installed in the bomb-bay of the aircraft for 0-g flights is shown in figure 2.

The basic system consisted of an expulsion cylinder, which stored the liquid mercury; a metering orifice, which measured the liquid mercury flow rate; heaters, which produced high-quality mercury vapor; a venturi nozzle, which measured mercury vapor flow rate; the condensing tube; a 1/16-inch orifice located at the condenser exit, which damped incipient oscillations of the liquid mercury leg in the condenser tube; and a receiver, which collected the condensed mercury.

Mercury flow was initiated and maintained by pressurizing the expulsion cylinder with nitrogen gas. In the 0-g system, a neoprene bladder was incorporated in the expulsion cylinder to control liquid mercury position during 0 g. The procedure for heating the mercury is as follows:

(1) A preheater was used to raise the liquid mercury to saturation temperature.

(2) A second heater partially boiled the liquid to approximately 25-percent quality.

(3) A third heater was designed to vaporize liquid drops in the vapor stream. This heater consisted of helical tubes followed by a packed bed of stainless-steel shavings.

Flow through the heaters produced superheated vapor with entrained liquid droplets; the vapor flow rate was generally about 90 percent of the total flow rate. The receiver was baffled to minimize movements of the liquid during the zero-gravity maneuvers.

The condensing tubes consisted of 0.41- and 0.44-inch constant-diameter low-alkali borosilicate glass tubes for the ground experiments and 0.27-, 0.40-, and 0.49-inch constant-diameter transparent high-silica glass tubes for the aircraft flights. The overall tube length for all tests was 87 inches. The condensing tube was cooled by gaseous nitrogen issuing uniformly in crossflow from two manifolds parallel to, and on opposite sides of, the tube.

Closeup photographs of the condensing flow were taken with a high-speed 16-millimeter motion-picture camera. In both facilities, the camera was mounted on rails that permitted it to be positioned anywhere along the length of the condenser tube. The camera framing rate was limited by the power supply available. In the aircraft, the framing rate reached approximately 4700 frames per second from the 120-volt supply; in the ground facility, larger power sources were available, 180 and 230 volts, permitting up to 5000 and 8000 frames per second, respectively. The optical system of the camera was modified by the incorporation of a four-sided rotating prism that recorded two images per frame - essentially doubling the framing rate. It was primarily the framing rate that determined the extent to which moving condensed drops could be detected. The framing

rate, then, determined the field of view of the condenser tube and the distance upstream of the interface where photographs could be taken. The locations of these stations are described more fully in the Procedure section. Illumination was provided by two 1000-watt lamps fixed at each station. Each lamp was mounted with a reflector specially designed to concentrate the light onto the desired portion of the tube.

In addition to the high-speed camera, a low-speed camera with a wide-angle lens was used in the aircraft to record the gross movement of the mercury interface during 0-g maneuvers. The vertical acceleration was indicated by an accelerometer that was in the field of view of the camera. The arrangement of the cameras is shown in figure 3.

Instrumentation

Oscillographs were used to record temperature and pressure data in both facilities. In the aircraft, the accelerations generated along the three axes of the aircraft (longitudinal, lateral, and vertical) were sensed by accelerometers located in the bomb-bay near the geometric center of the experiment. The accelerometers were used for aircraft control throughout the maneuver. The g-level indications were recorded on the oscillograph to provide a direct correspondence with system pressures. The oscillograph trace illustrated the time history of the 0-g maneuver starting from pullup to pullout. Following pullup, about 4 or 5 seconds of the initial trajectory were required to damp out pressure oscillations induced by the pullup maneuver. The portion of the trajectory during which the high-speed camera was operating was recorded by an oscillograph.

Stainless-steel inductance-type pressure transducers, capable of operating in a mercury environment up to 900° F, were used to measure venturi inlet absolute pressure and venturi pressure drip. Low-temperature transducers were used at all other locations in the system. Each transducer in direct contact with mercury was oriented so that its mounting tube and core axis were on the same horizontal plane as the condensing tube to minimize any mercury head effect. In addition, the mounting tube and core axis were positioned parallel to the lateral axis of the aircraft. Because the instrumentation was oriented in this manner and because acceleration is least in the lateral direction during the maneuver, the g effect of the mercury column in the pressure line was minimal.

Temperatures throughout the system were measured by ISA (Instrument Society of America) calibration K Chromel-Alumel thermocouples. A shielded, sheathed thermocouple was immersed in the mercury vapor stream in the venturi. At other locations, the thermocouple junction was spot welded to the outside surface of various components such as the heaters.

Procedure

Prior to each test, the mercury loop was evacuated to approximately 0.060 torr, and

the mercury heaters were brought to operating temperatures. Mercury vapor flow was initiated and maintained at a low rate for approximately 5 minutes to minimize the presence of noncondensables in the system. The receiver pressure was increased to a constant value (between 14 and 15 psia) and the gaseous nitrogen flow for condenser-tube cooling was regulated to locate the interface at the desired location. When a steady-state condition was achieved, the following data-recording procedures were used:

(1) In the ground facility, the oscillograph recorder was turned on. The high-speed camera was positioned and actuated at each of several stations (42, 55, and 68 in. downstream from the inlet) during a single setting of the flow rate through the 0.44-inch condenser tube. The framing rate was approximately 5800 frames per second. Data taken 6 inches downstream were obtained from films at approximately 8000 frames per second where the camera power source was 230 volts. The condenser tube used for this set of data was 0.41 inch inside diameter.

(2) In the aircraft, the condition for taking data at 1 g (level flight) was determined by the stability of the aircraft in all axes. At a signal from the pilot on attaining this condition, the oscillograph recorders and high-speed camera were turned on. The camera was located at the interface and 12 inches upstream from the interface, and operated at 4700 frames per second. Immediately prior to the actual zero-gravity maneuver, data recording was begun while still in level flight. The oscillograph recorders and the slow-speed, wide-angle-lens camera were turned on and operated throughout the entire maneuver. The interface was seen to undergo quite violent movements before stabilizing within the field of view of the camera. At this point of stabilization, when zero gravity was attained, the high-speed camera was turned on and operated through the camera reel capacity.

METHOD OF ANALYSIS

In the analysis of the photographic data, it was important to determine the conditions of flow into and through the mercury condenser.

Test Conditions and Measurement

Steady flow rate through the boiler was assumed. This assumption was based on tests of similarly designed boilers which indicated no holdup of the mercury flowing through them. The boiler outlet temperature was set to produce a superheated vapor to minimize liquid-mercury carryover. Although a venturi nozzle was installed to measure the vapor flow rate, the pressure transducer that measured the venturi differential pressure gave erratic readings. Reliable readings on subsequent tests, such as those de-

scribed in references 4 and 5, indicated that vapor quality ranged from 85 to 100 percent, but for most of the conditions, the quality was 90±5 percent. The condenser inlet pressures were based on a 90-percent recovery through the venturi nozzle. This value was quite accurate according to subsequent tests on the same nozzle. Inlet vapor velocities were calculated based on vapor flow rate at 90 percent of the total flow rate, on inlet pressure based on a 90-percent recovery through the venturi nozzle, and on vapor density determined by the superheated temperature.

Drop velocities and sizes were measured from the high-speed motion pictures by using the film framing rate and the length markers on the tube. Measurements requiring judgment, such as determination of an average velocity and a drop size, necessitated repeated viewing of the pertinent film sequences. Other measurements, such as determination of the highest drop velocity, required consideration of a number of drops to ensure their validity.

Vapor Velocity Distribution

The variation of vapor velocity along the length of a constant-diameter condenser tube depends mostly on the vapor-flow-rate variation along the condenser. This variation, in turn, is a function of the vapor quality and therefore dependent on the heat flux distribution of the condenser. If the condenser heat flux is constant and uniform over the condensing length, the quality decreases linearly with condensing length and would result in a linear decrease of vapor velocity. The test apparatus was constructed with cross-flowing gaseous nitrogen from two manifolds on opposite sides of the tube. This arrangement provided a constant and uniform heat sink along the condensing length. As long as vapor condensed on the entire tube surface within the condensing portion of the tube, a constant and uniform heat-flux condition would exist, and the vapor velocity would decrease linearly. With superheated vapor, heat transfer can conceivably be accomplished either (1) by convectively cooling the vapor to the saturation temperature in the initial part of the condensing tube and then by condensing the vapor thereon, or (2) by condensing throughout the condenser with a coexisting, superheated vapor core.

High-speed photographs indicated that mercury-vapor condensation began near the tube inlet in the presence of superheat. This observation agrees with the experimental data and analysis of condensation of superheated steam by Jakob (ref. 6). He established that the steam condensed on the tube wall even though the core of the vapor stream was at a superheated condition. The superheated steam persisted throughout the length of the test section. A similar observation was made by Kutateladze who expanded the analysis of Jakob by evaluating the heat transfer from the superheated core to the condensing layer of the vapor (ref. 7). The superheated mercury vapor, therefore, was expected to transfer heat according to the second alternative, described previously. The vapor velocity,

then, was regarded to vary linearly along the condensing length. In any case, the enthalpy difference due to the inlet superheat was small compared with the total condensation enthalpy change (approximately 6 percent) and would have a small effect on the velocity distribution.

RESULTS

The following discussion is based on observations of high-speed motion pictures of mercury condensing in constant-diameter glass tubes in the ground facility and in the aircraft. Photographs from the motion pictures are included in the discussion. The results, however, can be more clearly understood by viewing the film supplement.

Ground Facility

Motion pictures were taken at 6, 42, 55, and 68 inches downstream from the condenser inlet. The condensing length was kept at approximately 68 inches. A composite diagram of the forms that condensed mercury has taken is shown in figure 4. This diagram aids interpretation of the photographs in figure 5. The liquid-vapor interface is the beginning of a liquid-mercury leg that extends to the left (downstream). The condensed drops that are moving can only be distinguished by viewing the motion-picture sequence. The condensed drops moving on the wall are distinguished from those moving in the vapor stream by the streaks left in their paths. In all cases, the vapor-borne drops traveled at higher velocities than the moving drops on the wall. More detailed descriptions and explanations of these phenomena associated with mercury condensing flow are given in the discussion of the individual stations.

Observations. - Motion pictures of mercury vapor condensing 6 inches downstream from the inlet (fig. 5(a)) showed that within the range of drops that were visible, little of the condensed-liquid flow was accounted for by the drops in the vapor stream. The drops flowing on the wall appeared to account for the greater part of the total liquid flow rate. The path of the flowing drops on the wall was axial with a slight, but distinct, vertically downward component. The trajectory of the drops in the vapor stream, however, showed no vertical component. Condensation on the tube wall appeared as a mist that appeared to grow more dense with time. Most of the condensed drops on the wall were absorbed by large drops that had been formed upstream from this station. There were some areas of the wall, however, that remained relatively isolated from the flowing drops. Periodically, streaks appeared in the mist-like cover of condensed drops. These streaks were formed by drops that moved along the wall, agglomerated with other drops, and exposed bare tube surface. The size of these drops, measured by the width of the stream of the exposed tube surface as well as by a measurement of the drops themselves, was approxi-

mately 0.001 inch. These drops were seen either to continue moving in a halting manner along the wall, increasing in size (resulting from the wiping effect), or to be lifted into the vapor stream. Shortly thereafter, many other drops in the same area began moving. These drops absorbed other drops, combined with other moving drops, or were lifted into the vapor stream. In effect, the area was entirely wiped of the stationary condensed drops, thus exposing the bare tube surface. In time, the surface became covered with a mist-like cover again and the whole process repeated itself. The time required for 1 cycle was approximately 0.06 second.

At the station 42 inches from the inlet (fig. 5(b)), the amount of liquid flow in the vapor stream and on the wall was visibly greater than that at the inlet. The proportion of the flowing drops on the wall again was much greater than the drops borne by the vapor. The tendency toward downward movement of the drops on the wall and in the stream became more pronounced at this station compared with that at the inlet region. Large liquid accumulations resulting from agglomeration of wall run-off droplets were observed moving along on the tube bottom.

At the station 55 inches from the inlet (fig. 5(c)), the liquid flow rate in the vapor and on the wall was visibly greater than that observed at the previous station. The trajectories of the drops on the wall and in the vapor stream were steeper than those at previous stations. Thus, a denser concentration of drops resulted near the tube bottom. The larger drops on the wall generally moved at higher velocities than the smaller drops. Often, this higher velocity resulted in the smaller drops being absorbed by the larger ones. This action was most apparent for drops that moved along the tube bottom. When a drop reached a certain height, a portion of the drop appeared to be sheared away and sprayed into the vapor stream. The spraying sometimes occurred when a drop in the vapor stream collided with a drop moving on the wall. The most turbulent interactions between drops appeared to occur in this region of the tube.

The station 68 inches from the inlet (fig. 5(d)) was located in the immediate region of the interface. The liquid flow rate, in the form of moving drops, therefore, constituted virtually the total flow rate. The steep, downward trajectories of the drops in the stream and on the wall continued the trend established at the earlier stations resulting in a concentration of drops in the lower part of the tube. Part of this flow was in the form of large drops moving along the tube bottom. The interface was seen occasionally as a tongue of liquid extending into view. On impact with the drops moving along the tube bottom, the tongue of liquid appeared to be forced back downstream. The result of the impact often caused a bridging of the tube (sometimes termed slug flow).

A typical sequence of events at the interface and the immediate region behind it is shown in figure 6. Initially, the interface was a shallow, sloping surface due to the effect of gravity. Evidence of bridging, which evidently occurred outside the camera viewing range, is seen as a buildup of liquid that entrapped a pocket of vapor. Collapse of the

pocket occurs when the entrapped vapor condenses. In the film sequence, the collapse caused the forward wall of liquid mercury to advance and fill the void. Once condensation was initiated, the collapse took place quickly. The time intervals shown in the sequence are typical.

Measurement. - The films indicated many different phenomena occurring simultaneously in a flow of condensing mercury vapor. Mercury drops, covering a wide range of sizes, were observed both on the wall and in the vapor stream traveling over a range of velocities. Drops were lifted from the wall into the vapor stream, as well as being deposited onto the wall from the flowing vapor. Nevertheless, an effort was made in this report to categorize some of the phenomena that are pertinent to two-phase flow analysis. Table I lists these categories in terms of velocities and sizes of the drops borne by the vapor, those on the wall (other than those on the tube bottom), and those that accumulated and travel on the tube bottom.

The data are grouped according to the distance downstream from the condenser inlet. As mentioned in the Procedure section, data taken 6 inches downstream from the condenser inlet were obtained during a single setting of the flow rate through a 0.41-inch-diameter tube. Data taken at other stations along the 68-inch condensing length were taken through a 0.44-inch-diameter tube for a range of flow rates. The flow rate through the 0.41-inch-diameter tube, however, was approximately the same as many of the flow rates through the 0.44-inch-diameter tube, as indicated in table I. The term velocity ratio, as used herein, refers to the ratio of a vapor-borne-drop velocity at a particular station to the vapor velocity at that station.

The motion pictures in the ground facility produced sufficient detail to show moving drops that developed on the wall and that, on some cases, became vapor borne. It is reasonable to expect, therefore, that there was no drop smaller than these (i.e., as small as 0.001-in. diam). For the framing and image-recording rates considered, velocities of 0.001-inch-diameter drops could have been detected up to approximately 150 feet per second.

The typical size of the drops in the vapor stream appeared to be fairly uniform at all axial stations throughout the condenser. In contrast, the velocities of these drops covered a wide range. In most cases, the maximum velocity was about twice the minimum. The observed average velocity decreased at longer distances from the condenser inlet.

The minimum, the maximum, and the observed vapor-borne-drop velocities for these runs where the inlet vapor velocity ranged from 139 to 168 feet per second are plotted in figure 7. These velocities are shown as a function of the distance ratio x/L, that is, the ratio of the observed station (distance from the inlet) to the condensing length. In addition, the vapor velocities based on a linear velocity decrease are shown as dashed lines. The vapor velocity where x/L approaches 1.0 is shown to approach zero. Although

TABLE I. - CHARACTERISTICS OF CONDENSING MERCURY FLOW IN GROUND FACILITY ALONG 68-INCH CONDENSING LENGTH

Distance from condenser inlet, in.	Tube diameter, in.	Flow rate, lb/sec		Vapor velocity, ft/sec		Drops in vapor stream					Drops on wall			Observed average velocity of drops on tube bottom, ft/sec
		Total	Vapor entering condenser	Inlet	Local	Range of velocity, ft/sec	Range of velocity ratios	Observed average velocity, ft/sec	Observed average velocity ratio	Typical size, in.	Velocity, ft/sec		Typical size, in.	
											Maximum	Observed average		
[a]6	0.415	0.040	0.036	168	153	26 to 75	0.17 to 0.49	56.5	0.37	0.007	10.0	4.0	0.008	None
						32.9 to 70.4	0.22 to 0.46	46.5	.30	.005	4.4	3.8	.007	None
						35.7 to 66	0.23 to 0.43	43.2	.28	.006	8.7	5.5	.011	None
[a]42	0.44	0.0381	0.0343	142	54.3	30.1 to 58.3	0.56 to 1.07	40	0.74	0.007	5.8	5.6	0.020	5.9
		.0373	.0336	139	53.1	29.0 to 98.2	0.55 to 1.85	44.8	.84	.008	(b)	(b)	(b)	(b)
		.0403	.0363	150	57.4	34.8 to 63.7	0.61 to 1.11	40.8	.71	.008	7.1	6.0	.023	6.3
[c]55	0.44	0.0380	0.0342	142	27.2	22 to 34	0.81 to 1.25	25.2	0.93	0.007	8.3	4.0	0.014	2.2
		.0372	.0335	139	26.6	23.8 to 32.6	0.90 to 1.23	24.2	.91	(b)	(b)	(b)	(b)	(b)
		.0278	.025	104	19.9	13.4 to 29.8	0.67 to 1.50	20.9	1.05	.006	12.5	8.5	.017	9.9
		.0403	.0363	150	28.7	20.2 to 47.3	0.70 to 1.65	33.8	1.18	.014	9.7	4.4	.019	4.5
[c]68	0.44	0.0385	0.0347	142	≈0	6 to 13.0	>>1	12.1	>>1	0.010	4.9	3.6	0.014	5.0
		.0373	.0336	139	≈0	15.2 to 25.0	>>1	21.2	>>1	.006	(d)	(d)	.022	(e)
		.0530	.0477	197	≈0	17.0 to 29.1	>>1	20.1	>>1	.014	(d)	(d)	.026	(e)

[a]Most of liquid flow rate on wall.

[b]Drops on wall too blurry to take data.

[c]About half the liquid flow rate on wall.

[d]Drops on wall fall nearly vertically (negligible axial velocity).

[e]Not in view.

there may be recirculation eddies of vapor near the interface and it is expected that the interface surface itself serves as a condensation surface, these effects are expected to be small enough to be negligible. The range of the vapor-borne-drop velocities near the inlet ($x/L \cong 0.09$) is not shown to be too different from the velocities farther downstream. The maximum drop velocity at any station was measured at the station $x/L = 0.62$ (98 ft/sec). Although this velocity was that of a single drop and measurements of other drops at this same station were substantially less than 98 feet per second, it did show the possibility of attaining a higher velocity at a station farther downstream. The general trend, though, as indicated by the observed average drops, is for a decreasing velocity at distances farther from the condenser inlet. These velocities, however, are substantially less than the vapor velocity for most of the condensing length. It only becomes equal to the vapor velocity at approximately three-fourths of the distance to the interface. From this station to the interface, the vapor-borne drop has a higher velocity than the vapor.

The vapor-borne-drop velocities are plotted as a ratio of the local vapor velocities in figure 8 for all the data included in table I. The curve drawn through the observed average points indicates small velocity ratios near the inlet (low value of x/L), but higher ratios at higher values of x/L. At the interface, where the vapor velocity approaches zero, the curve becomes asymptotic. The curve indicates a value of about 0.3 at the inlet and reaches a value of 1.0 at about three-fourths of the condensing length.

The drops on the wall moved at a fairly uniform average velocity along the entire condensing length. The maximum velocities of the drops on the wall varied from 4.4 to 12.5 feet per second, but they seemed to be independent of station along the condensing length. The sizes of the drops on the wall appear to depend on location; that is, smaller drop sizes were nearer to the condenser inlet. In all cases, the typical drop size on the wall was greater than that borne by the vapor. The drop velocity on the tube bottom was in the same general range as the drop velocity observed at other circumferential locations on the wall.

Zero-Gravity Facility

High-speed motion pictures were taken at two locations along the 60-inch condensing length; one located at the interface and the other located 48 inches downstream from the inlet. Photographs at these locations were taken in the aircraft test installation under both 1- (level flight) and 0-g conditions. These sections of the condensing tube are characterized by low vapor quality and velocity. It would therefore be expected that the effects of gravity environment on droplet paths and trajectories would be most noticeable at these locations.

Observations. - The following observations compare the effects of gravity for several values of tube diameter. For a given mass flow rate, variation in tube diameter necessarily implies variation in fluid velocity. Although one's intuition more readily relates liquid-drop motion to vapor velocity than to tube diameter, vapor velocity is an inferred quantity that varies both axially and radially within the tube; on the other hand, tube diameter is a directly measured quantity that is little affected by subjective interpretation. For this reason, the following discussion is presented in terms of tube diameter. To aid his intuitive understanding of the related constituent processes, the reader may recall that, in general, vapor velocity is inversely proportional to the square of tube diameter.

At the station 12 inches from the interface (approximately 80 percent of the condensing length from the inlet), there was virtually no difference in the appearance of condensing mercury flow through the 0.27-inch-diameter tube between 1 and 0 g for the range of flow rates investigated (figs. 9(a) and (b) are typical photographs). In both cases, there appeared to be no localized drop concentration either on the wall or in the vapor stream. Flow through the 0.40-inch-diameter tube indicated some evidence of the effect of gravity on the drops, as shown in figure 9(c) and (d). There was a distinct concentration of drops on the tube bottom at 1 g, whereas the flow at 0 g showed uniform distribution of drops both on the walls and in the vapor stream. This tendency toward concentration of drops on the tube bottom is shown most distinctly for flow through the 0.49-inch-diameter tube in 1 g. A typical photograph showing not only the drops on the tube bottom, but also the vertical path of a condensed drop moving on the wall is presented in figure 9(e). Motion pictures were initially taken of the flow through the 0.49-inch-diameter tube at the interface; however, the tube breakage during pullup maneuvers became so frequent thereafter that further attempts to conduct flow observation studies in the 0.49-inch-diameter tube were discontinued.

The interface for all conditions was positioned at approximately 60 inches from the inlet. Flow through the 0.27-inch-diameter tube at this location showed some effect of gravity on the condensed drops (figs. 19(a) and (b)) in contrast to the location 12 inches upstream that showed no visible effect. Although there were drops throughout the vapor stream, there was a concentration of drops on the bottom that induced an undercut appearance of the interface. Again, the 0-g condition showed a uniform distribution of drops but with relatively larger drops on the wall. Flow through the 0.40- and 0.49-inch-diameter tubes (figs. 19(e) to (f)) showed the sharpest contrast of the effect of gravity on the condensed drops. At 1 g, practically all the flow of condensed drops was concentrated into a few, large, well-defined drops moving on the tube bottom. A large sloping interfacial area was exposed because of the leveling influence of gravity. The interface became periodically turbulent as a result of the impact of the moving drops. At 0 g, the drops again showed no localization of drop concentration. The interface at 0 g was essentially vertical.

TABLE II. - CHARACTERISTICS OF CONDENSING MERCURY FLOW IN AIRCRAFT ZERO-GRAVITY FACILITY

[Condensing length; 60 in.]

(a) 80 Percent of condensing length

Tube diameter, in.	Flow rate, lb/sec		Vapor velocity, ft/sec		Observed average velocity, ft/sec			Observed average velocity ratio
	Total	Vapor entering condenser	Inlet	Local	Vapor-borne drops	Drops on wall	Drops on tube bottom[a]	
				1 g				
0.27	0.0315	0.0284	325	65	27.3	6.5	7.4	0.42
	.0437	.0393	354	71	34.8	9.4	---	.49
	.0502	.0451	378	76	34.1	8.3	---	.45
0.40	(b)	(b)	(b)	(b)	18.8	(c)	3.8	(b)
	0.0435	0.0391	213	43	19.4	3.3	4.8	0.45
	.0528	.0475	239	48	23.3	4.4	5.8	.48
0.49	0.0315	0.0284	127	25	5.1	(c)	5.2	0.20
	.0428	.0385	165	33	6.9	(c)	5.9	.21
	.0508	.0457	174	35	7.5	(c)	6.4	.21
				0 g				
0.27	0.0303	0.0273	312	62	24.9	4.8	---	0.40
	.0447	.0402	366	73	30.9	6.8	---	.42
	.0470	.0423	371	76	33.4	9.3	---	.44
0.40	0.0329	0.0296	195	39	19.0	3.3	---	0.49
	.0448	.0403	232	46	19.8	3.4	---	.43
	.0529	.0475	246	49	25.6	6.9	---	.52

[a] 1-g condition only.

[b] No value; total flow rate not obtained.

[c] No value; few or no moving drops observed.

Measurements. - The conditions under which motion pictures at a station were taken in the zero-gravity facility are given in table II. As mentioned in the section Description of Apparatus, the electrical source in the aircraft in flight supplied 120 volts to the camera. Because this voltage level meant a lower camera framing rate compared with that in the ground facility, and because of the difficulty in predetermining the interface position at 0 g due to maneuver loads, a camera lens was chosen that would extend the field of view to about 4 inches. As a result, motion pictures offered excellent observation of the contrast in behavior of the drops on the wall and the interface at 1 and 0 g. Under such conditions, however, the drops in the vapor stream and the smaller drops, in gen-

TABLE II. - Concluded. CHARACTERISTICS OF CONDENSING MERCURY FLOW IN AIRCRAFT ZERO-GRAVITY FACILITY

[Condensing length, 60 in.]

(b) Interface region

Tube diameter, in.	Flow rate, lb/sec		Inlet vapor velocity, ft/sec	Observed average velocity, ft/sec		
	Total	Vapor entering condenser		Vapor-borne drops	Drops on wall	Drops on tube bottom[a]
1 g						
0.27	0.0313	0.0282	328	11.1	1.8	5.8
	.0415	.0373	370	16.7	4.5	8.2
	.0512	.0460	364	12.6	5.0	8.6
0.40	0.0324	0.0292	165	7.4	(b)	1.5
	.0435	.0391	203	8.0	(b)	3.8
	.0529	.0475	222	9.2	(b)	3.1
0.49	0.0311	0.0280	124	(b)	(b)	2.4
	.0426	.0386	162	(b)	(b)	4.5
	.0511	.0460	168	(b)	(b)	3.7
0 g						
0.27	0.0355	0.0320	(c)	14.3	4.5	---
	.0426	.0384	320	14.8	7.5	---
	.0531	.0478	290	15.7	5.2	---
0.40	0.0315	0.0284	178	9.9	1.2	---
	.0435	.0391	214	13.7	2.7	---
	.0521	.0470	215	14.3	4.4	---
0.49	0.0283	0.0255	115	5.2	2.6	---
	.0430	.0387	172	13.1	3.2	---
	.0519	.0466	197	12.8	5.9	---

[a] 1-g condition only.

[b] No value; few or no moving drops observed.

[c] No value; vapor temperature not obtained.

eral, were much more difficult to detect and to measure compared with the results of the ground facility. The tabulations, therefore, consist of measurements of the velocity of the drops on the wall and on the tube bottom. Table II indicates that some measurements could not be made because few or no moving drops were observed. These conditions of low vapor velocity were brought about by a combination of low flow rate and large tube diameter. The vapor velocities resulted in a negligible drag force on the drops. Gravity, therefore, becomes the predominating influence. This resulted in large drops that rolled down the tube wall with virtually no axial component to the drop path.

At 0 g, however, and aside from the influence of the tube surface, the drops in one part of the tube were no different from the drops in any other part. Because there is no top or bottom at 0-g conditions, there was no need to differentiate the drop velocities on the tube bottom from the drop velocities on the tube wall. All drop velocities on the tube wall, therefore, were included in one category. The higher flow rates through the 0.27-inch-diameter tube at 1 g exhibited the same type of uniform concentration of drops as at 0 g. For these conditions, also (flow rate, 0.04 and 0.05 lb/sec), the category of drop velocities on the tube wall included all drops on the wall.

By considering these factors, a comparison of wall-borne-drop velocities between 1 and 0 g indicates a fairly close agreement. At the station 80 percent of the condensing length from the inlet, the range of drop velocities for the 0.27-inch-diameter tube was 6.5 to 9.4 feet per second at 1 g and 4.8 to 9.3 feet per second at 0 g. The velocities of both the drops on the wall and the drops on the tube bottom for flow in the 0.40-inch-diameter tube ranged from 3.3 to 5.8 feet per second at 1 g and from 3.3 to 6.9 feet per second at 0 g.

In the interface region, a more significant difference in the drop velocities on the wall, including those on the tube bottom, might be expected because of the proportionately greater effect of gravity. Generally, however, when the drop velocities at 1 and 0 g are compared for any given tube size, there is close agreement. For the flows in the 0.40-inch-diameter tube, the velocity in the tube bottom at 1 g ranged from 1.5 to 3.8 feet per second; at 0 g, the drops on the wall ranged from 1.2 to 4.4 feet per second. Comparable drop velocities for the 0.49-inch-diameter tube ranged from 2.4 to 4.5 feet per second at 1 g and 2.6 to 5.9 feet per second at 0 g. The drop velocities for flow in the 0.27-inch-diameter tube ranged from somewhat lower values at 1 g (1.8 to 8.6 ft/sec) compared with the values at 0 g (4.5 to 7.5 ft/sec).

Vapor and noncondensable gas pockets were visible within the liquid leg at 1 and 0 g. The vapor pockets were formed continually by the turbulence of the interface, but they collapsed quickly. One such sequence of a vapor pocket forming and collapsing at 0 g is shown in figure 11. Measurements at 0 g indicate that the vapor pocket extended into the liquid leg about 1/2 inch and the time interval between pocket formation to its collapse averaged about 0.04 second. This time interval agrees closely with the 0.05-second

interval obtained from the ground facility. The vapor and noncondensable pockets were more apparent at 0 g probably because the interfacial area was small compared with the 1-g case. The larger exposed interfacial area at 1 g provided a ready access for the entrapped noncondensable pockets to escape into the vapor region. Noncondensables were also seen in the form of small bubbles attached to the tube wall within the liquid leg. These bubbles remained stationary during the motion-picture sequence. The lowest flow rate, 0.0283 pound per second, flowing in the largest diameter tube, 0.49 inch, at 0 g (fig. 12), illustrates a vivid example of noncondensable gas behavior in the region immediately behind the interface. The motion-picture sequence shows this gas pocket continually forming and then escaping into the vapor region.

DISCUSSION OF RESULTS

Results from the photographic studies of the ground and zero-gravity facilities offer a more clear understanding of the flow regimes and of the values of pertinent parameters of two-phase mercury condensing flow.

It was apparent in the ground facility that, at all stations along the condenser tube, the moving drops on the wall tended to remain on the wall, while the vapor-borne drops tended to remain in the vapor stream. A moving drop on the wall had the effect of absorbing the stationary condensed drops in its path. Most of the stationary drops appeared to be removed from the tube surface in this manner. At least half of the liquid flow rate was a result of these moving drops. The drops that became entrained in the vapor stream (other than those due to the breakup of large drops) were those located in areas relatively isolated from the moving drops on the wall. These isolated areas were usually located at the top of the tube at 1 g, since the moving drops on the wall had a generally downward path due to gravity. At any measuring station, the larger drops moving on the wall were observed to travel at a higher velocity than the smaller ones. It was evident that the larger drops, extending farther into the vapor stream, were subject to greater drag forces than the smaller drops. As long as the drag force did not exceed the surface-tension force, the drop remained intact but was maintained at a high velocity. When the drag force exceeded the surface-tension force, part of the drop sheared away and sprayed into the vapor stream. This is one aspect of the critical drop size that is discussed more fully in reference 8.

At 0 g, the moving drops did not have a downward path but, instead, traveled axially. This motion had the effect of wiping the entire surface area frequently. This wiping effect accounts for the relatively clear appearance of the glass condensing tube at 0 g compared with the cloudy appearance at 1 g. One would expect, therefore, that the areas on the tube surface isolated from the mobing drops and from which drops might be entrained into the vapor stream would be substantially reduced. As a result, fewer drops would

have been expected in the vapor stream in a 0-g condition compared with a 1-g condition. The motion pictures at 0 g had inadequate resolution to confirm this expectation.

The effect of gravity on the path of the moving drops on the wall and on the trajectory of the vapor-borne drops was noticeable. Toward the interface, these drops tended to accumulate into large drops on the tube bottom. Under the conditions in the ground facility, this concentration of drops resulted in highly turbulent interactions between the vapor and the large drops at the tube bottom, and also between individual drops. At 0 g, no such accumulations of drops occurred, and for the conditions imposed, no such region of high turbulence was observed. In contrast to the visual differences, the observed average velocity of the moving drops on the condenser wall ranged between comparatively narrow limits (1 to 9 ft/sec) at all the measuring stations of 1- and 0-g conditions. This can be attributed to the self-compensating factors of the generally smaller drops in the higher velocity region experiencing the same drag force as the larger drops in the lower vapor velocity region of the condenser.

The velocity of the drops in the stream varied over a wide range, even at a particular station along the condensing length. Consideration of the observed average velocity at the different stations in the ground facility, showed that the drop velocity in the stream was lower than the vapor velocity for most of the condensing length, varying from 0.3 to 1.0 of the local vapor velocities at the inlet and at three-fourths of the condensing length, respectively.

The results of the study imply that the mechanism of flowing vapor dropwise condensation is different in many respects from what has been conceived. The implications are enumerated as follows:

(1) Much of the liquid is on the wall either as moving drops or as stationary condensing drops - the amount depends on the local quality. A generalized correlating parameter that is based on smooth-wall friction factors is not as valid as that which accounts for changes in local effective wall roughness. This effect may be expected to be different at 1 g and at 0 g, depending on the difference of drop distribution.

(2) The assumption of constant velocity ratio in pressure-drop correlations is not rigorously valid because the ratio of vapor-borne-drop velocity to vapor velocity varies with the location within the condensing length (in the ground facility the velocity ratio varied from 0.3 to $>>1.0$).

(3) The interface in a horizontally oriented tube is more stable at 0 g than at 1 g.

(4) With a reasonable liquid leg in the condensing tube (not less than about 3 in.), the probability of vapor carryover beyond the condenser outlet is remote.

(5) The moving drops on the wall absorb the stationary condensed drops in their paths and expose the bare tube surface for condensing. Improved heat transfer is therefore expected in 0 g, where the uniform distribution of drops on the wall provides a frequent and continuous exposure of the tube surface to the vapor.

CONCLUSIONS

For mercury flowing at the rate of 0.03 to 0.05 pound per second through glass tubes ranging from 0.27 to 0.49 inch in diameter, and with the condensing length at 60 or 68 inches, the following conclusions were reached:

Ground Facility:

1. At all stations along the condensing length, moving drops on the wall contributed an estimated one-half or more of the liquid flow rate.

2. The observed average velocity ratio (ratio of the observed average vapor-borne drop velocity to the local vapor velocity) varied from 0.3 at the inlet to 1.0 at approximately three-fourths of the condensing length from the inlet.

3. The observed average velocity of the moving drops on the wall was approximately constant over the entire condensing length and ranged between 1 and 9 feet per second.

4. Vapor pockets were observed within the liquid leg. The time interval between pocket formation and its collapse averaged about 0.05 second.

Zero-Gravity Facility:

1. Flow distribution in the 0.27-inch-diameter tube at 0 g was similar to that observed at 1 g.

2. Flow at 1 g in the 0.40- and 0.49-inch-diameter tubes was characterized by a concentration of drops along the tube bottom and a nearly horizontal interface; at 0 g, the drops on the wall were distributed uniformly and the interface was essentially vertical. There was no localization of drop concentration in the stream or on the wall at 0 g; the interface was stable and vertical.

3. In general, gravity level had negligible effect on the velocity of the drops on the wall (including those on the tube bottom).

4. Vapor pockets were observed within the liquid leg at 1 and 0 g. The time interval between pocket formation and its collapse averaged about 0.04 second at 0 g.

Lewis Research Center,
National Aeronautics and Space Administration,
Cleveland, Ohio, January 12, 1967,
120-33-07-03-22.

APPENDIX - AJ-2 ZERO-GRAVITY FLIGHT FACILITY

The AJ-2 airplane (fig. 13) that was used for the test flights is a converted Navy attack bomber powered by two reciprocating engines and one jet engine. The aircraft was modified to assure fuel and oil supply to the engines during the 0-g flights. The only other necessary modification was the addition of structure for mounting the test package semirigidly to the aircraft.

A typical trajectory flown during the investigation is shown in figure 14. This maneuver produces a theoretical maximum 0-g time of 24 seconds. The maneuver was entered from a dive and the airplane was rotated at 400 knots true airspeed to arrive at a pitch angle of 42° with a speed of 310 knots true airspeed. Transition was made from a nominal 2-g pullup rotation to the 0-g condition where the aircraft was flying on a Keplerian trajectory. Approximately 5 or 6 seconds were required for transition from the pullup to the 0-g condition, and a similar time was required at the exit of the Keplerian curve to pullup. These transition times reduce the theoretical maximum 0-g time to a practical time of 12 to 14 seconds.

The 0-g times obtained for this study were adequate because flow stabilization times in the experimental system were of the order of 4 to 5 seconds following the initial pullup maneuver.

The quality of the 0-g condition produced in the aircraft should be considered on the basis of the three axes of measurement. However, the lateral and longitudinal accelerations always had a better quality than the vertical acceleration. The vertical accelerations for a typical trajectory are shown in figure 15. During this maneuver, approximately 2 seconds were achieved at a level of 0.005 g or less, while approximately 19 seconds were achieved at a level less than 0.1 g.

All the maneuvers flown during the test program were analyzed, and average 0-g times were computed. From these data, for an average of approximately 5 seconds per trajectory, the g level was within ± 0.01 g, and for approximately 13 seconds, the g level was within ± 0.05 g.

Flights were made in a restricted airspace over Lake Erie because of the possibility of an inadvertent mercury spillage. The aircraft was monitored on radar for separation from stray aircraft, and continuous radio contact was maintained with NASA Flight Operations as an added precaution. On initial flights, a chase aircraft was flown with the AJ-2 to observe any possible external malfunctions or system leakages.

REFERENCES

1. Lockhart, R. W.; and Martinelli, R. C.: Proposed Correlation of Data for Isothermal Two-Phase, Two-Component Flow in Pipes. Chem. Eng. Progr., vol. 45, no. 1, Jan. 1949, pp. 39-48.

2. Baroczy, C. J.; and Sanders, V. D.: Pressure Drop for Flowing Vapors Condensing in a Straight Horizontal Tube. Rep. No. NAA-SR-6333, Atomics International Div., North American Aviation, Inc., June 1, 1961.

3. Koestel, Alfred; Gutstein, Martin U.; and Wainwright, Robert T.: Study of Wetting and Nonwetting Mercury Condensing Pressure Drops. NASA TN D-2514, 1964.

4. Albers, James A.; and Macosko, Robert P.: Experimental Pressure-Drop Investigation of Nonwetting, Condensing Flow of Mercury Vapor in a Constant-Diameter Tube in 1-G and Zero-Gravity Environments. NASA TN D-2838, 1965.

5. Albers, James A.; and Macosko, Robert P.: Condensation Pressure Drop of Nonwetting Mercury in a Uniformly Tapered Tube in 1-G and Zero-Gravity Environments. NASA TN D-3185, 1966.

6. Jakob, Max: Heat Transfer in Evaporation and Condensation - II. Mech. Eng., vol. 58, no. 11, Nov. 1936, pp. 729-739.

7. Kutateladze, S. S. (S. J. Rimshaw, trans.): Heat Transfer in Condensation and Boiling. AEC TR-3770, 1952, pp. 53-60.

8. Sturas, Jonas I.: Mercury Droplet Size and Distribution in Glass Condenser Tube in 1-g and Zero-Gravity Environments. NASA TM X-1338, 1967.

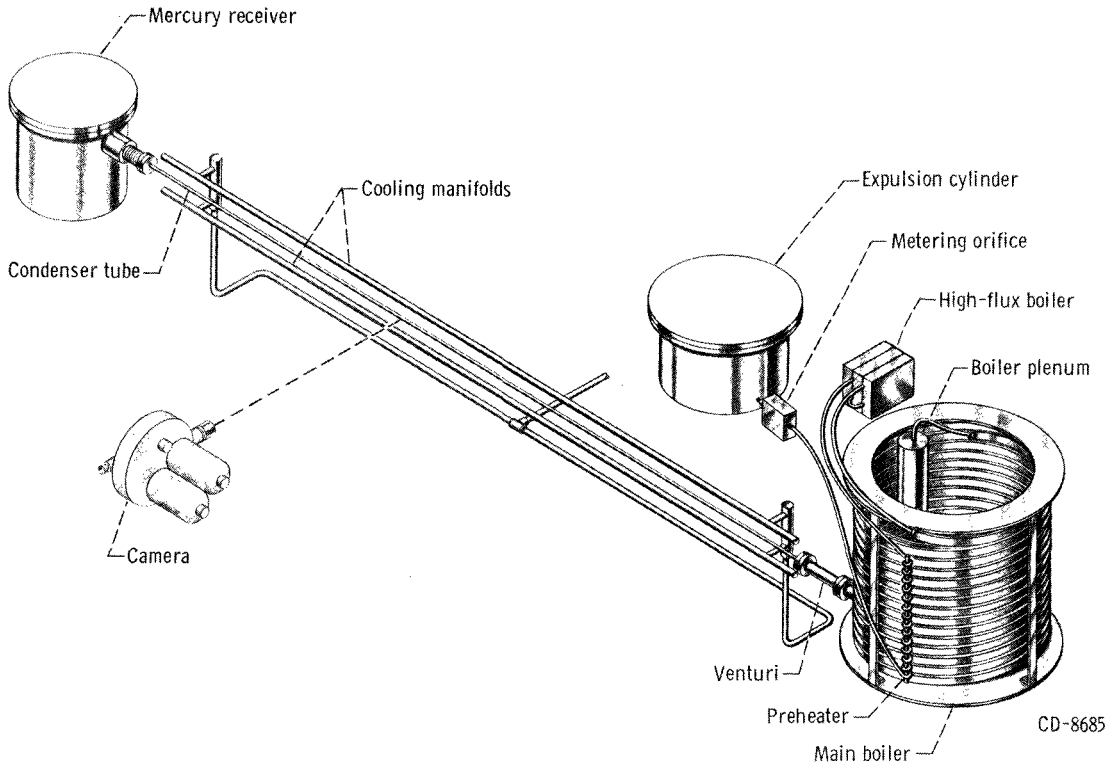

(a) Isometric drawing of experimental system.

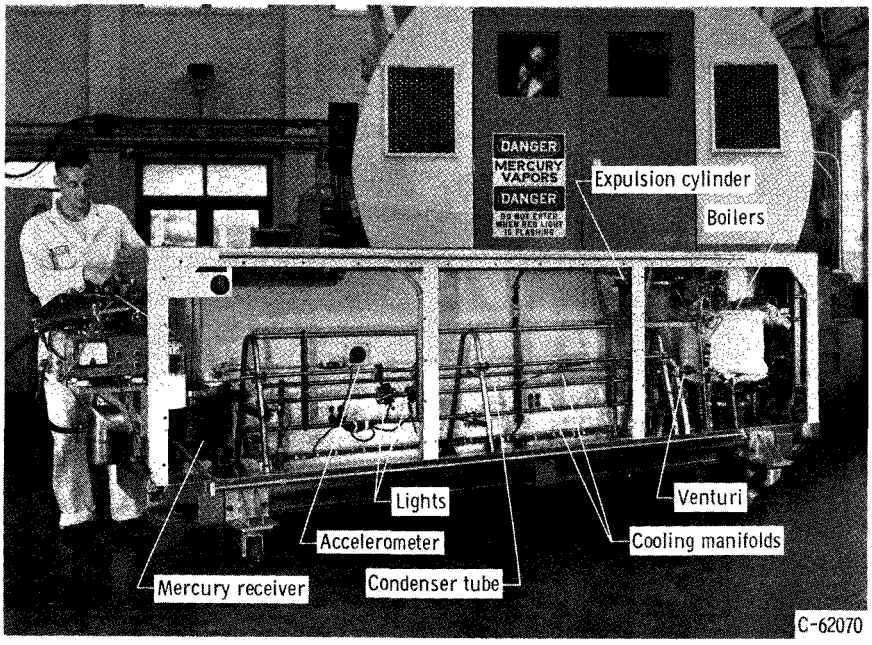

(b) Actual view of experimental system in aluminum enclosure.

Figure 1. - Basic mercury condensing system.

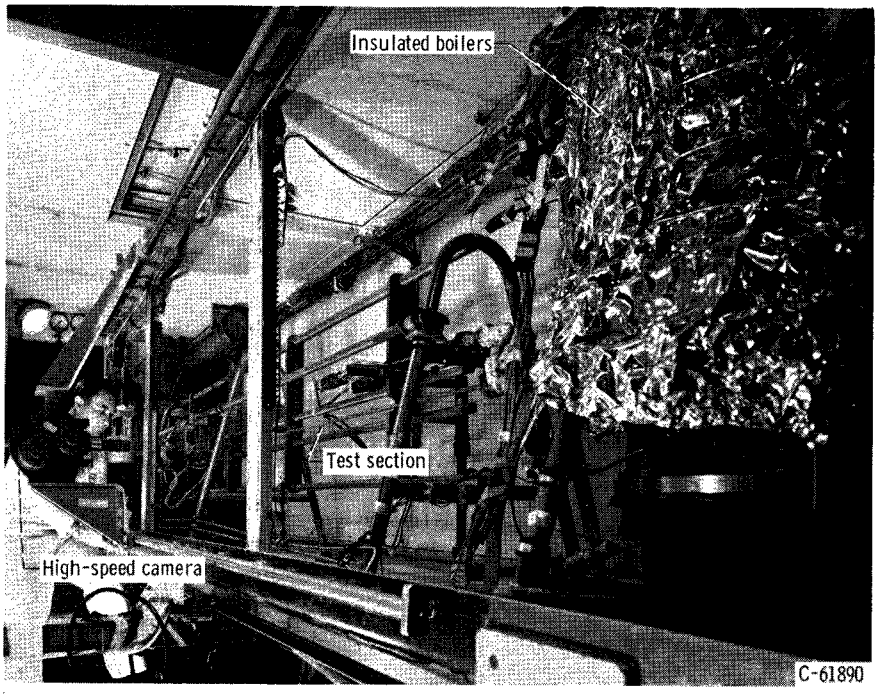

Figure 2. - Experimental package installed in aircraft (boiler end).

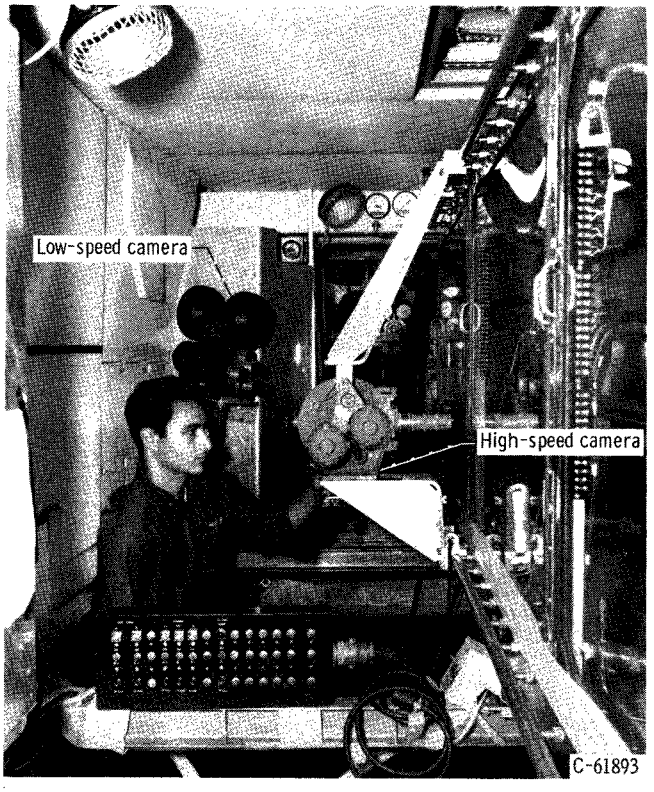

Figure 3. - Cameras in position in 0-g aircraft facility.

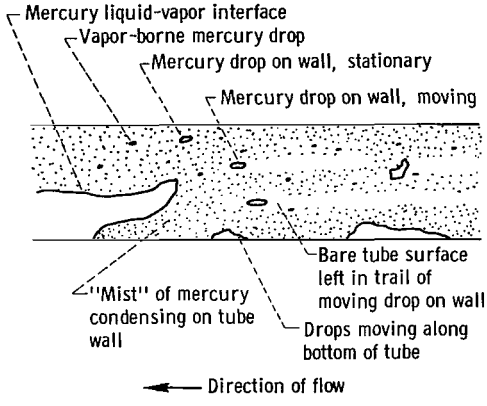

Figure 4. - Composite diagram of liquid-mercury condensation.

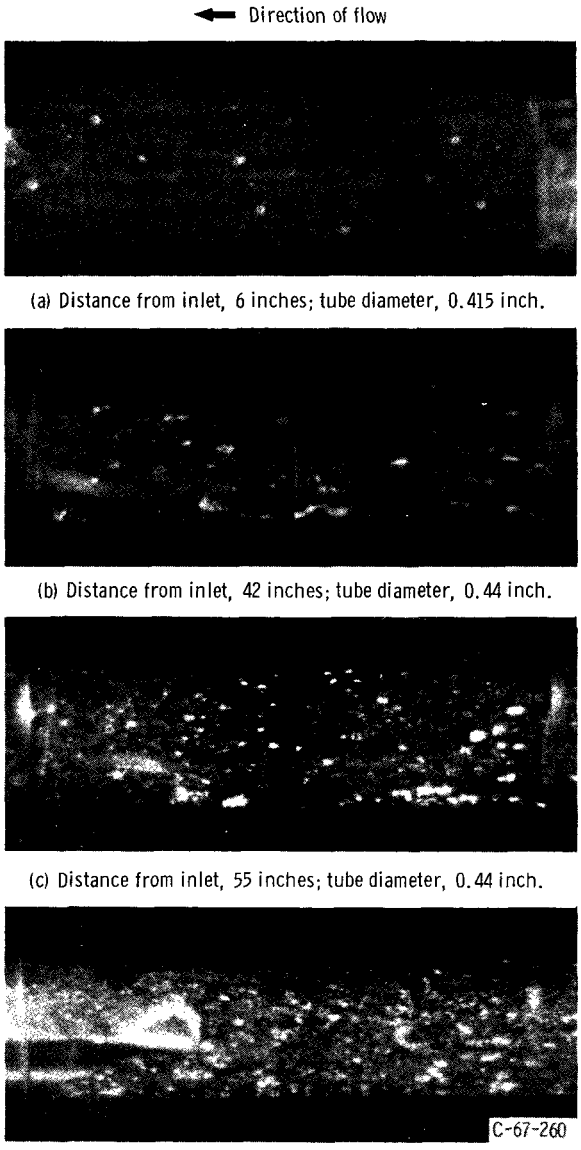

(a) Distance from inlet, 6 inches; tube diameter, 0.415 inch.

(b) Distance from inlet, 42 inches; tube diameter, 0.44 inch.

(c) Distance from inlet, 55 inches; tube diameter, 0.44 inch.

(d) Distance from inlet, 68 inches; tube diameter, 0.44 inch.

Figure 5. - Mercury condensation at various stations along glass tube. Condensing length, 68 inches.

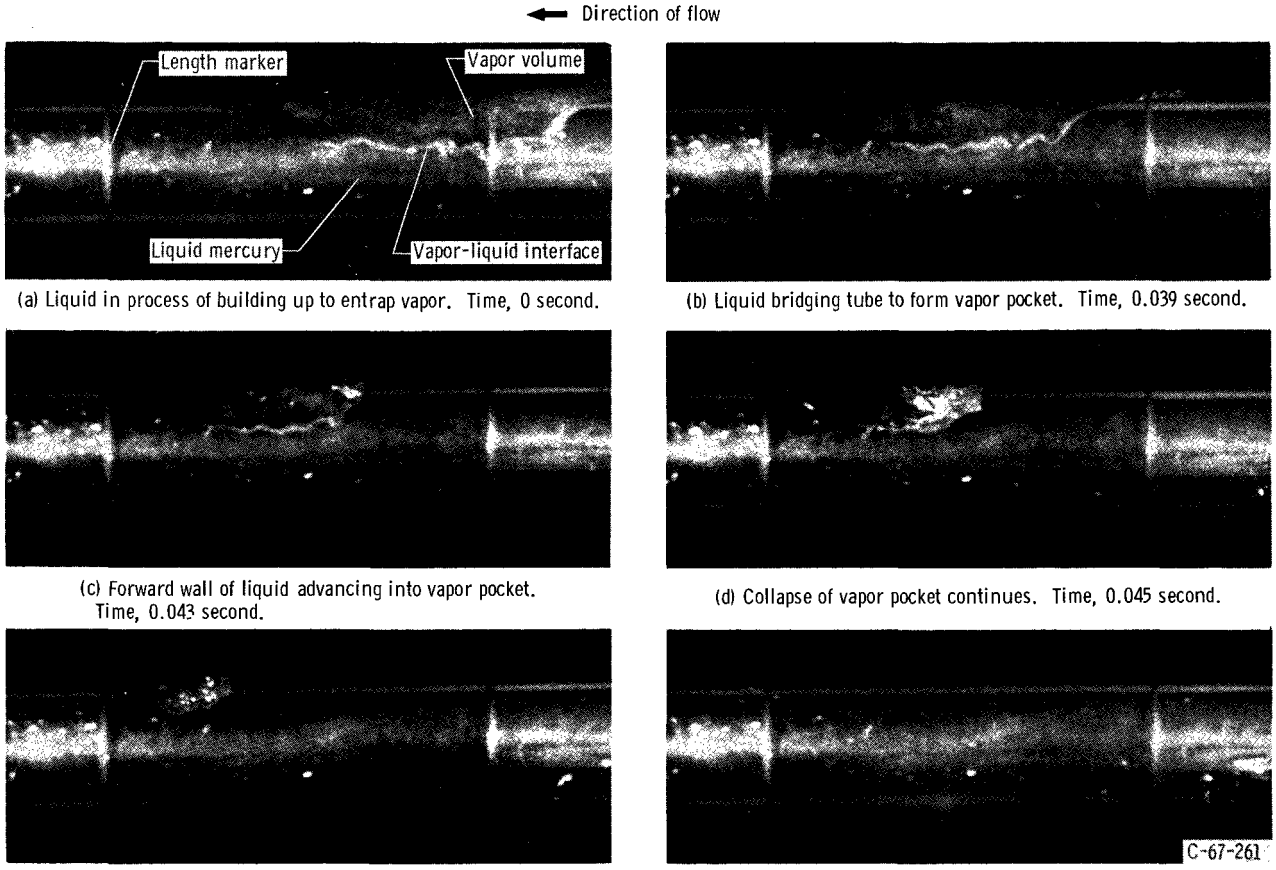

(a) Liquid in process of building up to entrap vapor. Time, 0 second.

(b) Liquid bridging tube to form vapor pocket. Time, 0.039 second.

(c) Forward wall of liquid advancing into vapor pocket. Time, 0.043 second.

(d) Collapse of vapor pocket continues. Time, 0.045 second.

(e) Collapse almost complete. Time, 0.050 second.

(f) Collapse completed. Time, 0.053 second.

Figure 6. - Formation and collapse of vapor pocket in mercury condensing tube.

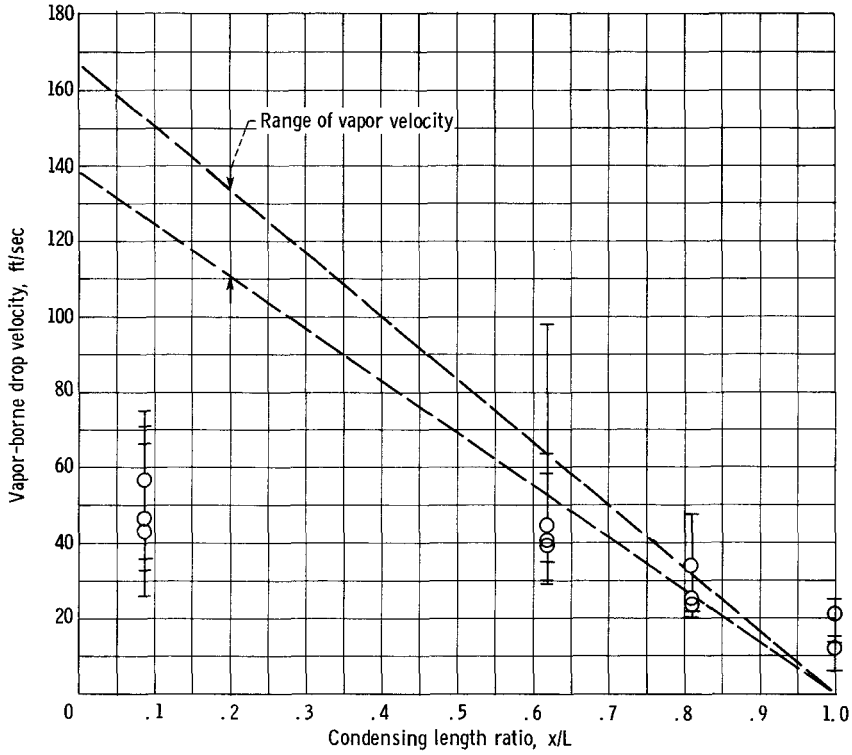

Figure 7. - Vapor-borne velocities at stations along condensing length for ground facility. Inlet vapor flow rate, 0.033 to 0.036 pound per second; condensing length, 68 inches.

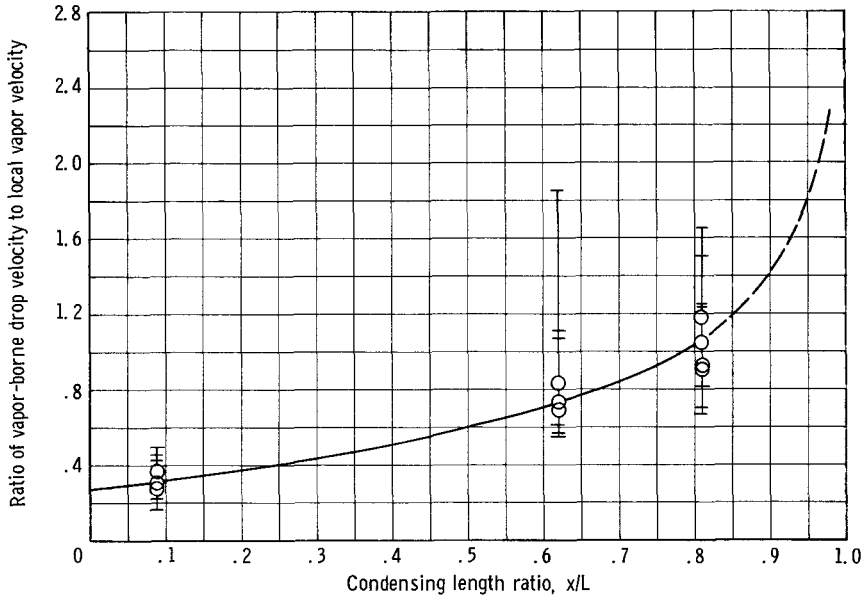

Figure 8. - Variation of velocity ratio (vapor-borne drop to local vapor) with condensing length ratio for ground facility. Total flow rate, 0.028 to 0.040 pound per second; condensing length, 68 inches; inlet velocity, 104 to 168 feet per second.

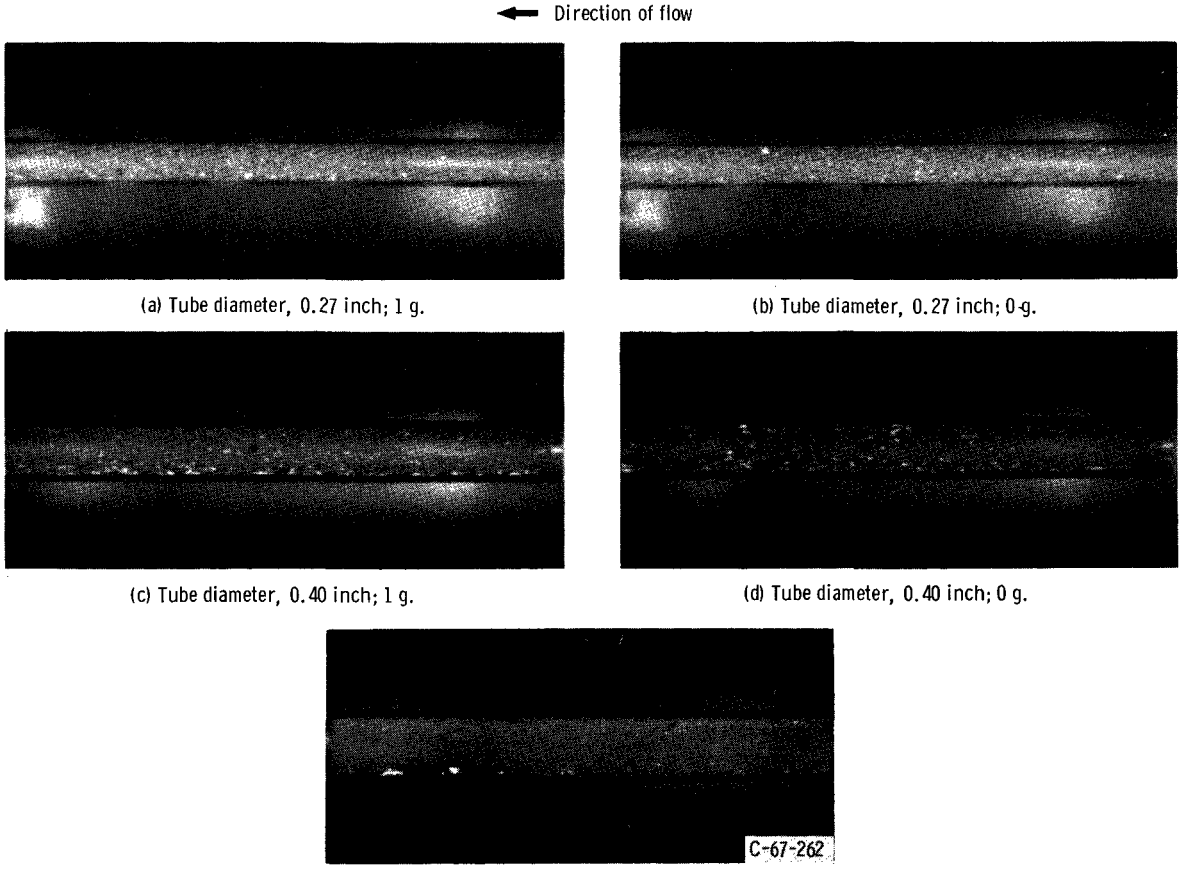

(a) Tube diameter, 0.27 inch; 1 g.

(b) Tube diameter, 0.27 inch; 0 g.

(c) Tube diameter, 0.40 inch; 1 g.

(d) Tube diameter, 0.40 inch; 0 g.

(e) Tube diameter, 0.49 inch; 1 g.

Figure 9. - Condensing mercury vapor flow in vapor region. Flow rate, 0.043 pound per second.

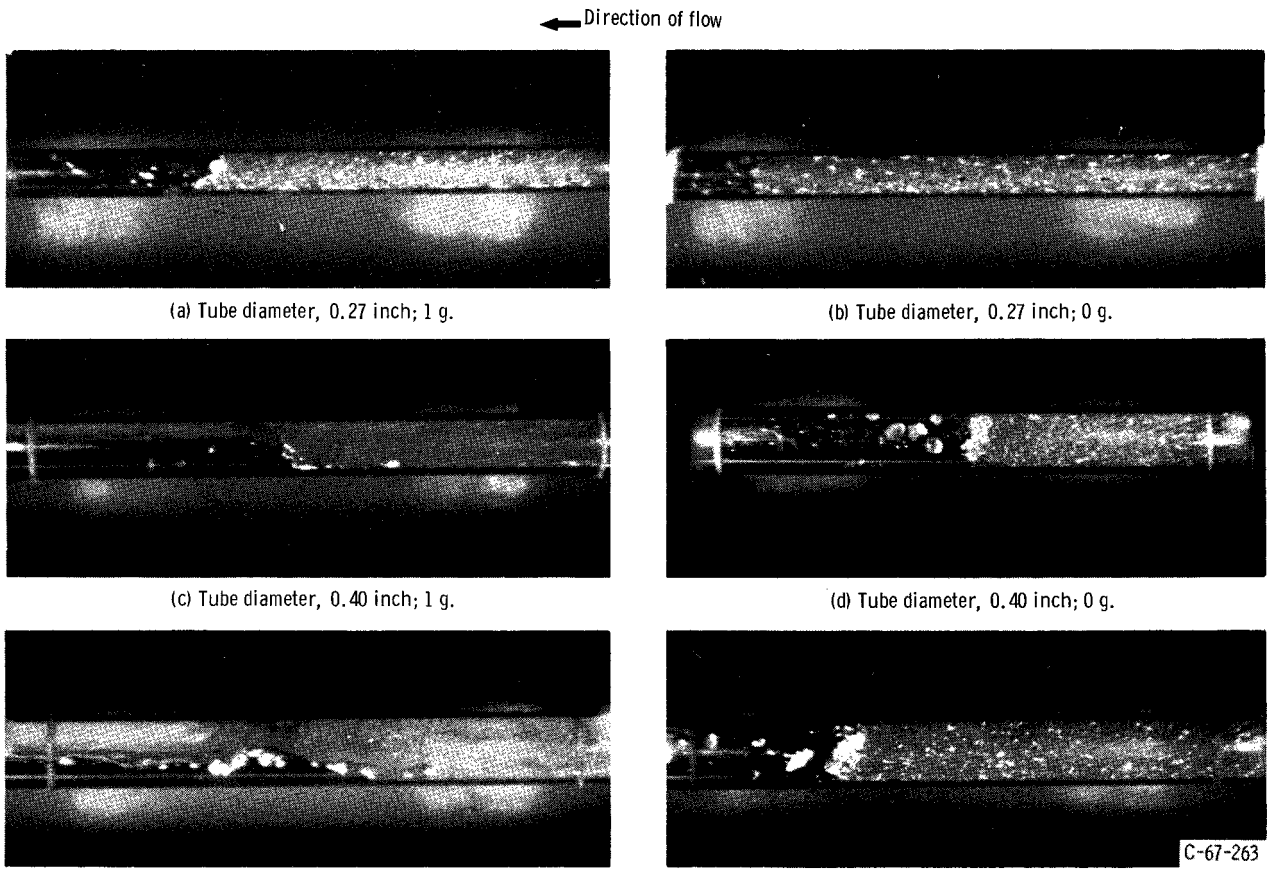

(a) Tube diameter, 0.27 inch; 1 g.

(b) Tube diameter, 0.27 inch; 0 g.

(c) Tube diameter, 0.40 inch; 1 g.

(d) Tube diameter, 0.40 inch; 0 g.

(e) Tube diameter, 0.49 inch; 1 g.

(f) Tube diameter, 0.49 inch; 0 g.

Figure 10. - Condensing mercury vapor flow at interface. Flow rate, 0.052 pound per second.

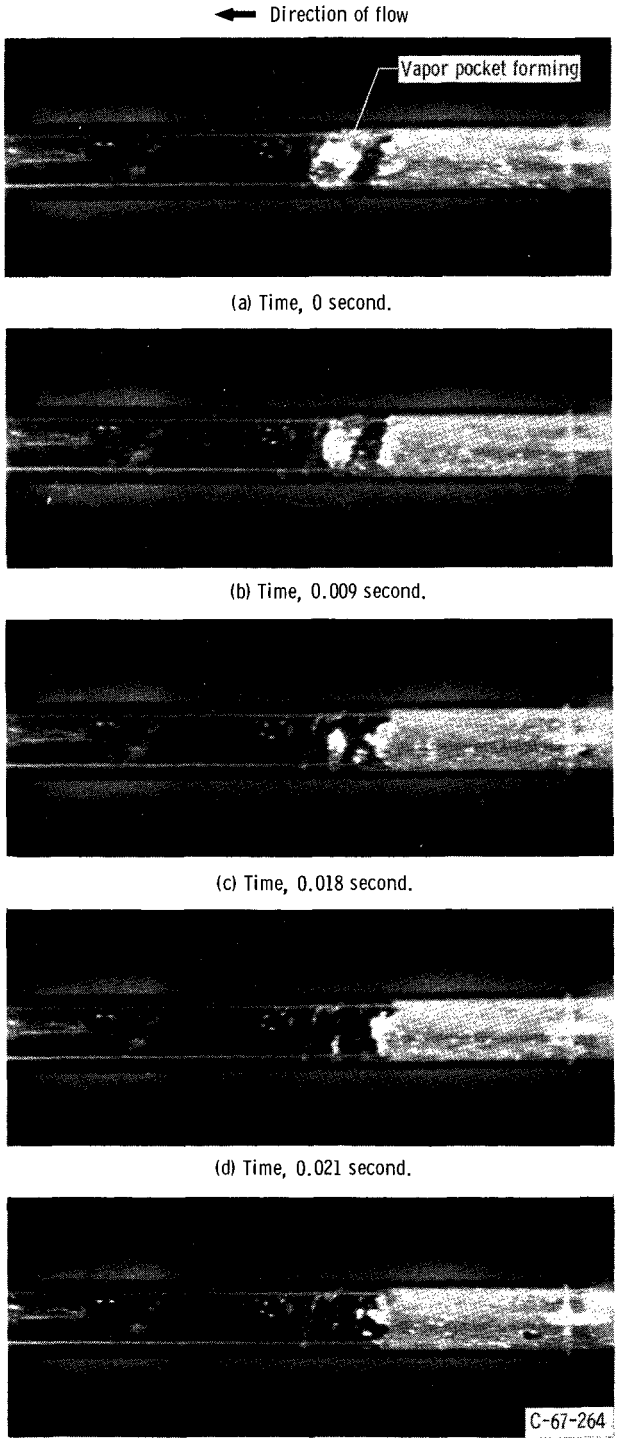

(a) Time, 0 second.

(b) Time, 0.009 second.

(c) Time, 0.018 second.

(d) Time, 0.021 second.

(e) Time, 0.027 second; vapor pocket collapsed.

Figure 11. - Formation and collapse of mercury vapor pocket at 0 g. Flow rate, 0.031 pound per second; tube diameter, 0.40 inch.

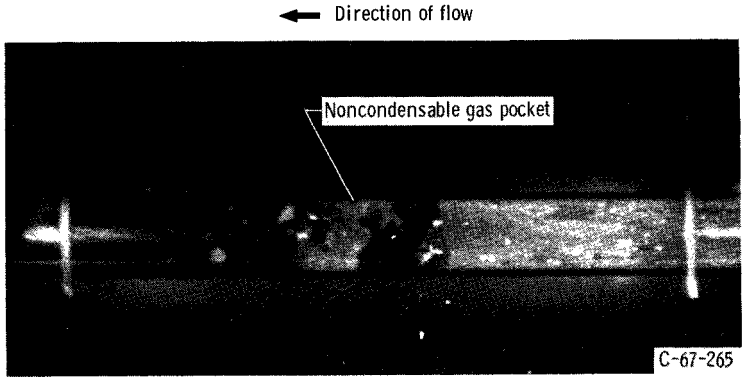

Figure 12. - Condensing mercury vapor flow in 0.49-inch-diameter tube at 0 g showing noncondensable gas pocket behind interface.

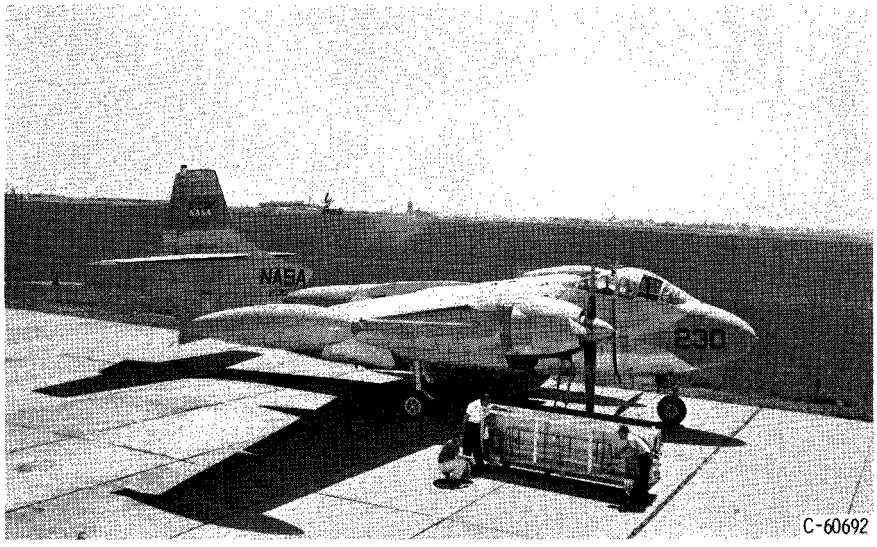

Figure 13. - AJ-2 aircraft 0-g flight facility.

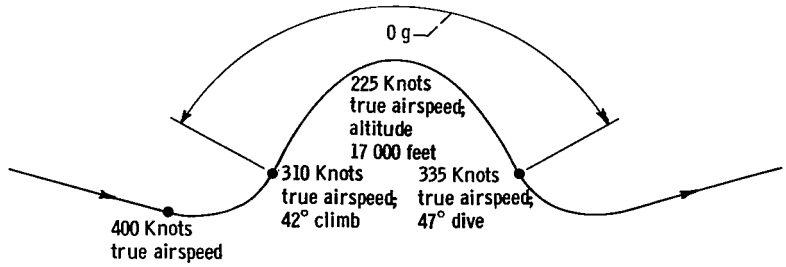

Figure 14. - Typical trajectory. Actual 0-g time, 12 to 14 seconds; theoretical maximum overall time, 24 seconds.

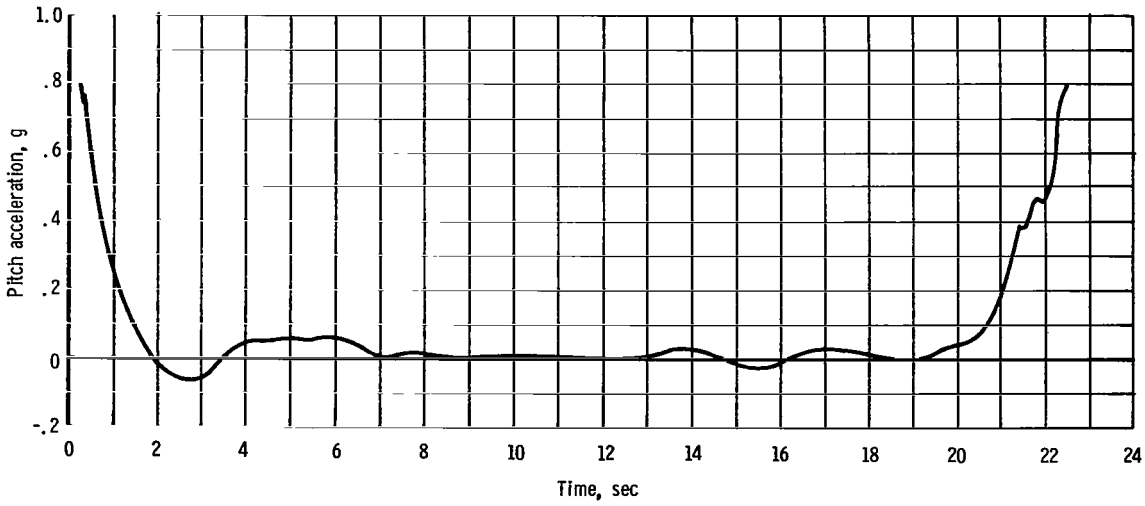

Figure 15. - Pitch acceleration during typical trajectory.

Motion Picture Film Supplement C-251 and Lewis Motion Picture (C 221) are available on loan. Requests will be filled in the order received. You will be notified of the approximate date scheduled.

Film Supplement C-251 (16 mm, 20 min, black and white, sound) is a study of condensing mercury flow at 1 and 0 g that uses high-speed motion picture sequences extensively. Results include those obtained in both the ground facility and the aircraft zero-gravity facility.

Lewis Motion Picture C-221 (16 mm, 12 min, color, sound), part of the mercury evaporating-condensing-analysis (MECA) project, includes an introduction to space power systems, a description of the MECA - AJ-2 flight package and associated hardware, and high-speed film sequences of mercury condensing in 1- and 0-g environments.

Film Supplement C-251 and Lewis Motion Picture C-221 are available on request to:

Chief, Technical Information Division (5-5)
National Aeronautics and Space Administration
Lewis Research Center
21000 Brookpark Road
Cleveland, Ohio 44135

CUT

Date _____

Please send, on loan, copy of ( ) Film Supplement C-251 to
TN D-4023 Lewis Film C-221.

_____
Name of Organization

_____
Street Number

_____
City and State Zip code

Attention: Mr. _____
Title _____

"The aeronautical and space activities of the United States shall be conducted so as to contribute . . . to the expansion of human knowledge of phenomena in the atmosphere and space. The Administration shall provide for the widest practicable and appropriate dissemination of information concerning its activities and the results thereof."

—NATIONAL AERONAUTICS AND SPACE ACT OF 1958

NASA SCIENTIFIC AND TECHNICAL PUBLICATIONS

TECHNICAL REPORTS: Scientific and technical information considered important, complete, and a lasting contribution to existing knowledge.

TECHNICAL NOTES: Information less broad in scope but nevertheless of importance as a contribution to existing knowledge.

TECHNICAL MEMORANDUMS: Information receiving limited distribution because of preliminary data, security classification, or other reasons.

CONTRACTOR REPORTS: Scientific and technical information generated under a NASA contract or grant and considered an important contribution to existing knowledge.

TECHNICAL TRANSLATIONS: Information published in a foreign language considered to merit NASA distribution in English.

SPECIAL PUBLICATIONS: Information derived from or of value to NASA activities. Publications include conference proceedings, monographs, data compilations, handbooks, sourcebooks, and special bibliographies.

TECHNOLOGY UTILIZATION PUBLICATIONS: Information on technology used by NASA that may be of particular interest in commercial and other non-aerospace applications. Publications include Tech Briefs, Technology Utilization Reports and Notes, and Technology Surveys.

Details on the availability of these publications may be obtained from:

SCIENTIFIC AND TECHNICAL INFORMATION DIVISION

NATIONAL AERONAUTICS AND SPACE ADMINISTRATION

Washington, D.C. 20546